Finite-size effect on the Raman-active modes of double-walled carbon nanotubes

2008 J. Phys.: Condens. Matter 20 015204

(http://iopscience.iop.org/0953-8984/20/1/015204)

J. Phys.: Condens. Matter **20** (2008) 015204 (5pp) doi:10.1088/0953-8984/20/01/015204

Finite-size effect on the Raman-active modes of double-walled carbon nanotubes

K Sbai[1], A Rahmani[1,3], H Chadli[1] and J-L Sauvajol[2]

[1] Equipe de Physique Informatique et Modélisation des Systèmes, Université MY Ismail, Faculté des Sciences, BP 11201, Zitoune, 50000 Meknès, Morocco
[2] Laboratoire des Colloides, Verres et Nanomatériaux (UMR CNRS 5587), Université Montpellier II, 34095 Montpellier Cedex 5, France

Received 27 July 2007, in final form 4 October 2007
Published 29 November 2007
Online at stacks.iop.org/JPhysCM/20/015204

Abstract
The dependence of the breathing-like phonon modes (BLM) and tangential-like phonon modes (TLM) of individual, finite and infinite bundles of double-walled carbon nanotubes (DWCNTs) as a function of the relative lengths of the inner (L_i) and outer (L_o) tubes is calculated by using the spectral moments method in the framework of the bond-polarization theory. Depending on the relative lengths of the inner (L_i) and outer (L_o) tubes, additional modes are evidenced in the BLM region. These modes must be considered in the analysis of the experimental data.

1. Introduction

Carbon nanotubes [1] have become a standard material in nanotechnology and a variety of applications using nanotubes have been proposed for investigation. Single-walled carbon nanotubes (SWCNTs) have been intensively studied during the past decade. One of the most important subjects for nanotube technology is to characterize nanotubes in a simple and quick way. Among the techniques extensively used to characterize these materials, Raman spectroscopy provides important information regarding both the electronic and the phonon spectrum of carbon nanotubes [2]. To derive this information, the Raman data have been correlated with theoretical predictions [3–5]. In this context, in the framework of the bond-polarization theory and using the spectral moments method [6, 7], we previously calculated the nonresonant polarized Raman spectra of both chiral and achiral SWCNTs as a function of the tube diameter and length [8].

Double-walled carbon nanotubes (DWCNTs), which consist of two concentric cylindrical graphene layers, are synthesized by a catalytic chemical vapor deposition method (CCVD) [9–11] and by thermal conversion of fullerene C_{60} encapsulated in SWCNTs [12]. Phonons in DWCNTs have been extensively investigated by Raman scattering [13–17]. In this context, the Raman responses of infinite DWCNTs have been calculated in the framework of the bond-polarization theory, using the spectral moments method [18]. Relations have been derived which describe the dependence of the radial breathing-like mode (RBLM) frequencies with the diameter of the inner and outer tubes. It was found that the frequencies in the breathing-like mode (BLM) and tangential-like mode (TLM) regions of DWCNTs significantly differ from those calculated for single-walled carbon nanotubes. For diameters of inner tubes (D_i) and outer tubes (D_o) in the range 0.6–2.2 nm and 1.2–3.2 nm, respectively, we found, unlike the expressions in [18], that the diameter dependence frequencies of the in-phase (low-frequency component: ω_{LF}) and out-of-phase (high-frequency component: ω_{HF}) RBLM was described by the following relations:

$$\omega_{LF}\ (\mathrm{cm}^{-1}) = -734.3/D_i + 118.1/D_i^2 + 946.1/D_o + 564.8/D_o^2 \quad (1)$$

and

$$\omega_{HF}\ (\mathrm{cm}^{-1}) = 128.0 + 188.6/D_i - 300.0/D_o + 295.6/D_o^2. \quad (2)$$

These expressions well describe the diameter dependence of both RBLMs in the range investigated. As expected for infinite diameters, the in-phase mode, which correspond to a transverse acoustic mode, has a zero frequency and the out-of-phase mode, which correspond to the breathing mode of a bilayer of graphene, has a frequency of 128 cm^{-1}, close to that of the B_{2g} graphite phonon mode [19].

In this paper we extend our previous study by considering DWCNTs with inner and outer tubes of different lengths. Indeed, some experiments show short portions of inner tubes inside outer tubes. Contrary to that, after different treatments, inner tubes can go beyond outer tubes. Because these different structures exist in a real sample, we calculate the nonresonant Raman spectra of individual and bundled DWCNTs consisting

[3] Author to whom any correspondence should be addressed.

of (n, n) inner and $(n + 5, n + 5)$ outer nanotubes of different lengths. We found that the low-frequency spectrum of the DWCNT is strongly sensitive to the relative lengths of the inner (L_i) and outer (L_o) tubes. These predictions are useful for interpreting the experimental Raman spectra of DWCNTs.

2. Model and method

In DWCNTs the inner and outer tubes are assumed to be at a distance close to 0.34 nm ± 10%. The relation between the diameters of the inner (D_i) and outer (D_o) tubes is $D_o = D_i + 2d$. The diameter of a (n, m) tube is given by $D = a[3(m^2 + mn + n^2)]^{1/2}/\pi$, with $a = 0.142$ nm. The previous relation determines the possible inner tubes (n, m) for a specific external tube (k, l), leading to a $(n, m)@(k, l)$ DWCNT. The $(n, n)@(n + 5, n + 5)$ DWCNTs satisfy this relation. Homogeneous bundles of finite size are formed by DWCNTs placed parallel to each other on a finite-size hexagonal array of cells of parameter $a_0 = D_o + d_{t-t}$, with the intertube spacing d_{t-t} fixed to 0.32 nm. The number of double tubes per bundle is denoted N_t.

The intratube interaction is represented by the force constants set used in our previous paper concerning the Raman spectrum of SWCNTs [8]. A Lennard-Jones potential, $U_{LJ} = 4\epsilon[(\sigma/R)^{12} - (\sigma/R)^6]$, describes the intertube interactions for both SWCNT–SWCNT and DWCNT–DWCNT interactions. The van der Waals parameters, $\epsilon = 2.964$ meV and $\sigma = 0.3407$ nm, are used in all our calculations. For the different DWCNTs investigated, the Lennard-Jones intertube interaction energy was minimized with respect to the interlayer separation, the relative angle of rotation of the layers around the tube axis and their relative translation along the tube axis. The optimal intertube gap is found to be around 0.34 nm. Calculations of the Raman spectrum, before and after energy minimization, do not show significant difference in the mode frequencies. This result was in agreement with that of Popov [20, 21] who found no significant differences between the BLM and TLM frequencies of the optimized and non-optimized DWCNTs in terms of relative angles of rotation and relative translation of the inner and outer tubes.

Nonresonant Raman spectra are calculated by using the spectral moments method in the framework of the bond-polarization theory (for details see [8, 16, 18]). The spectral moments method is described in detail in [6, 7]. It was successfully used to describe the vibrations of several systems [6–8, 18, 22–24]. Applying this method to calculate the low-frequency vibrations (smaller than 10 cm^{-1}) of very large systems presents some difficulties. As shown in our earlier works, a sharp truncation of the continued fraction leads to the appearance of sharp lines in the calculated low-frequency spectrum. On the other hand, the calculations of Raman and infrared spectra show that a limited number of moments are sufficient to obtain the frequency of modes with a good accuracy. In this work 500 moments have been used. The intensity of the Raman spectrum is normalized with respect to the number of carbons in the sample under consideration. The Raman active-mode frequencies are obtained from the position of the peaks in the calculated Raman spectra (the linewidth of each peak was fixed at 1.7 cm^{-1}). In our calculations, the common axis of the inner and outer tubes is along the Z axis, and a carbon atom of each tube is along the X axis of the DWCNT reference frame. The laser beam is kept along the Y axis of the reference frame. To calculate the polarized ZZ spectra, both incident and scattered polarizations are along the Z axis of the tubes.

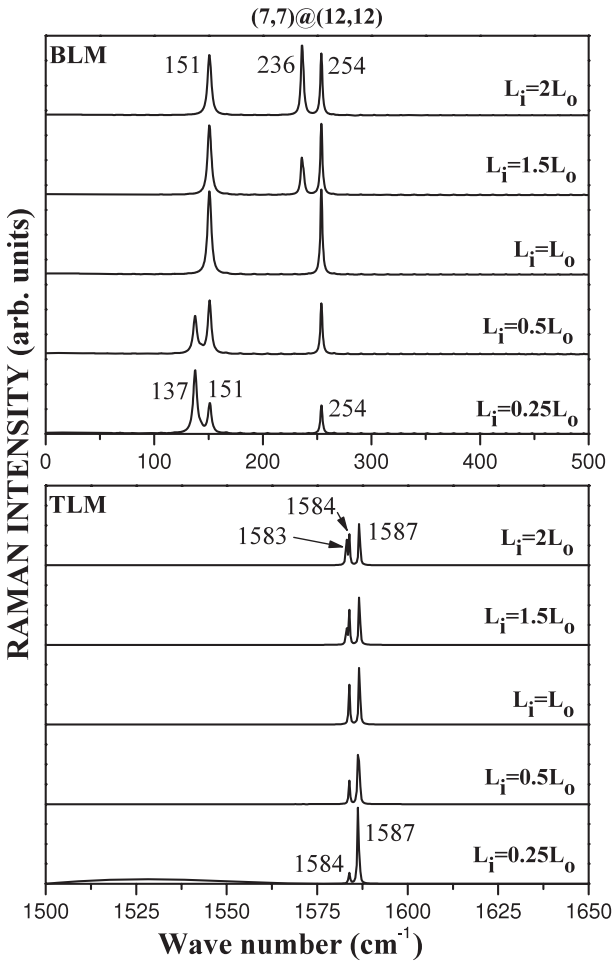

Figure 1. The calculated ZZ Raman spectra of (7, 7)@(12, 12) DWCNTs as a function of the ratio L_i/L_o in the BLM (top) and TLM (bottom) regions.

3. Results and discussion

In this work, the dependence of the Raman spectrum of $(n, n)@(n + 5, n + 5)$ DWCNTs (individual and bundle) as a function of the relative lengths of the inner (L_i) and outer (L_o) tubes is mainly investigated.

3.1. Individual DWCNTs

In figure 1 we report the dependence of the BLM (on the top) and TLM regions (on the bottom) of the Raman spectrum of (7, 7)@(12, 12) DWCNT as a function of the L_i/L_o ratio ($L_i/L_o = 0.25$, 0.5, 1, 1.5 and 2). For usual DWCNTs ($L_i = L_o$), the BLM range is dominated by two peaks located around 151 cm^{-1} and 254 cm^{-1} assigned to the in-phase and

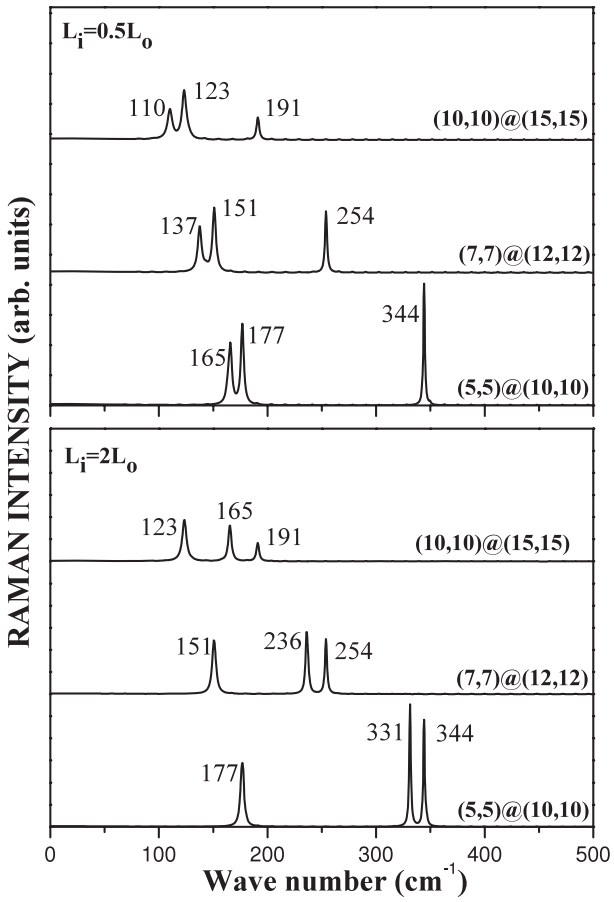

Figure 2. Dependence of the BLM range of (5, 5)@(10, 10), (7, 7)@(12, 12), and (10, 10)@(15, 15) DWCNTs for $L_i = 0.5L_o$ (top) and $L_i = 2L_o$ (bottom).

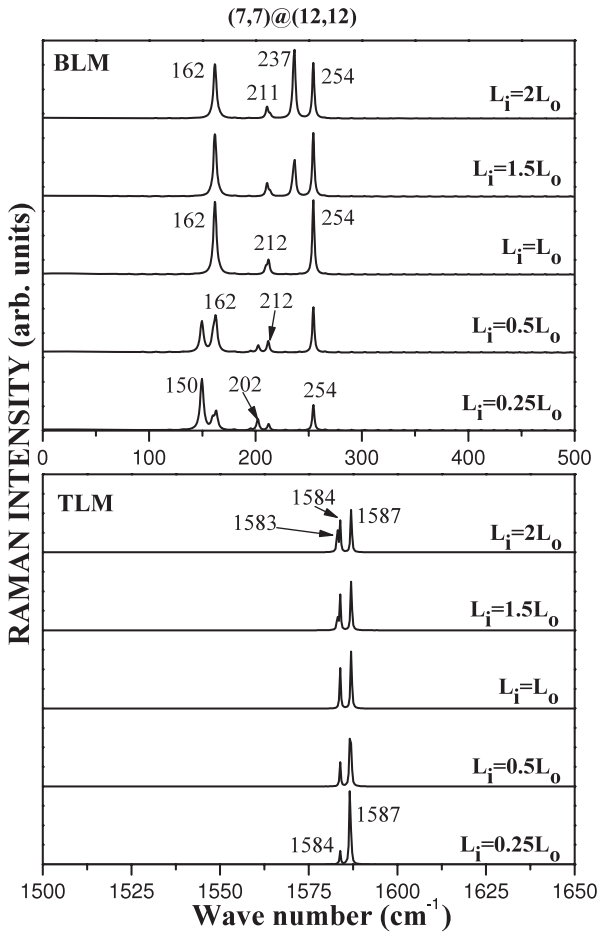

Figure 3. Polarized ZZ Raman spectra of (7, 7)@(12, 12) DWCNT crystals as a function of the ratio L_i/L_o in the BLM (top) and TLM (bottom) regions.

out-of-phase RBLMs, respectively. For $L_i < L_o$, an additional low-frequency peak around 137 cm^{-1} is observed and assigned to the radial breathing mode of the part of the outer tube which does not interact with the inner tube. Conversely, for $L_i > L_o$, the additional peak around 236 cm^{-1} is assigned to the radial breathing mode of the part of the inner tube which does not interact with the outer tube. The frequencies of both these additional modes are the same as those of the RBM of the (12, 12) and (7, 7) SWCNTs, respectively. As expected, all RBLM modes are upshifted by comparison with the RBM of the related single tubes: (i) for $L_i < L_o$ the low-frequency RBLM shifts by $\Delta\omega_{LF} = 14$ cm^{-1} and (ii) for $L_i > L_o$ the high-frequency RBLM shifts by $\Delta\omega_{HF} = 18$ cm^{-1}. These shifts do not depend on the L_i/L_o ratio. Experimentally, the measurement of the BLM region allows to detect differences in the length of the inner and outer tubes.

By contrast, the TLM region slightly depends on the L_i/L_o ratio. The TLMs are calculated at 1584 and 1587 cm^{-1} in the (7, 7)@(12, 12) DWCNT (figure 1). For $L_i > L_o$, an additional component at 1583 cm^{-1} is observed and assigned to the tangential mode (TM) of the part of the inner tube which does not interact with the outer tube (the TM of the (7, 7) SWCNT is calculated at the same position [18]). For $L_i < L_o$, the additional TM, featuring the part of the outer tube which does not interact with the inner tube, overlaps with the TLM at 1587 cm^{-1}. With regard to the slight sensitivity of the TM region to the relative lengths of the inner and outer tubes, its measurement gives no information about these lengths. Consequently, in the following we focus on the dependence of the BLM region on the relative lengths of the inner and outer tubes.

We were interested in the dependence of the spectra on the diameter of DWCNTs with inner and outer tubes of different lengths. Figure 2 shows the BLM region of the calculated Raman spectra of (5, 5)@(10, 10), (7, 7)@(12, 12) and (10, 10)@(15, 15) DWCNTs for $L_i = 0.5L_o$ (top) and for $L_i = 2L_o$ (bottom). All the Raman spectra show three modes: two modes result from the in-phase and out-of-phase coupled motions of breathing modes of the inner and outer tubes and the other mode originates from the RBMs of the individual walls. For the smallest tube, (5, 5)@(10, 10), each of the two RBLMs with frequencies of 177 and 344 cm^{-1} has similar features to the RBM of the related single layer (165 and 331 cm^{-1}). The reason is that the frequencies of the RBMs of the separate layers differ significantly from each other and, consequently, the mixing of both modes is negligible [25]. In contrast, for the largest tube (10, 10)@(15, 15), due the closeness of the RBM frequencies of the two single layers (110 and 165 cm^{-1}, respectively), the low- and high-frequency RBLMs located at

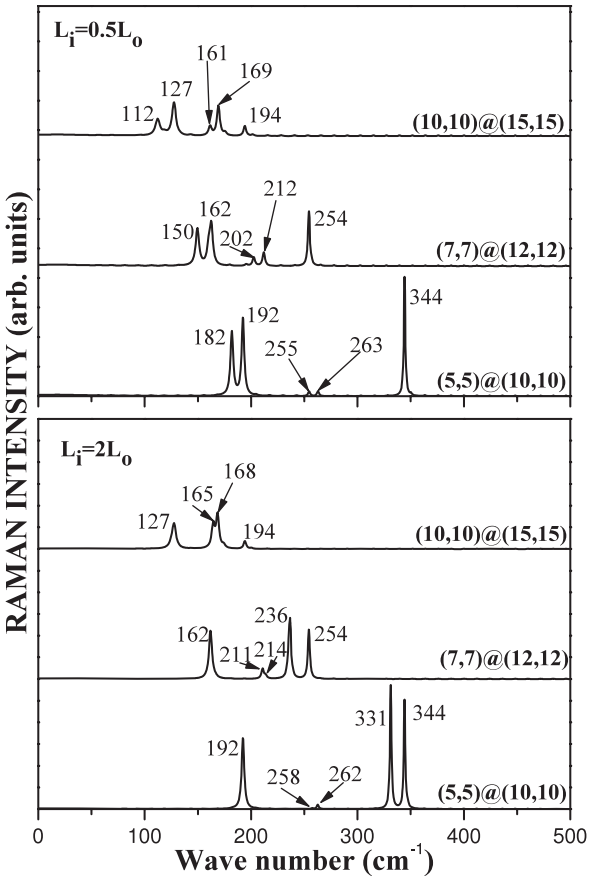

Figure 4. Dependence of the BLM range of (5, 5)@(10, 10), (7, 7)@(12, 12), and (10, 10)@(15, 15) DWCNT crystals for $L_i = 0.5L_o$ (top) and $L_i = 2L_o$ (bottom).

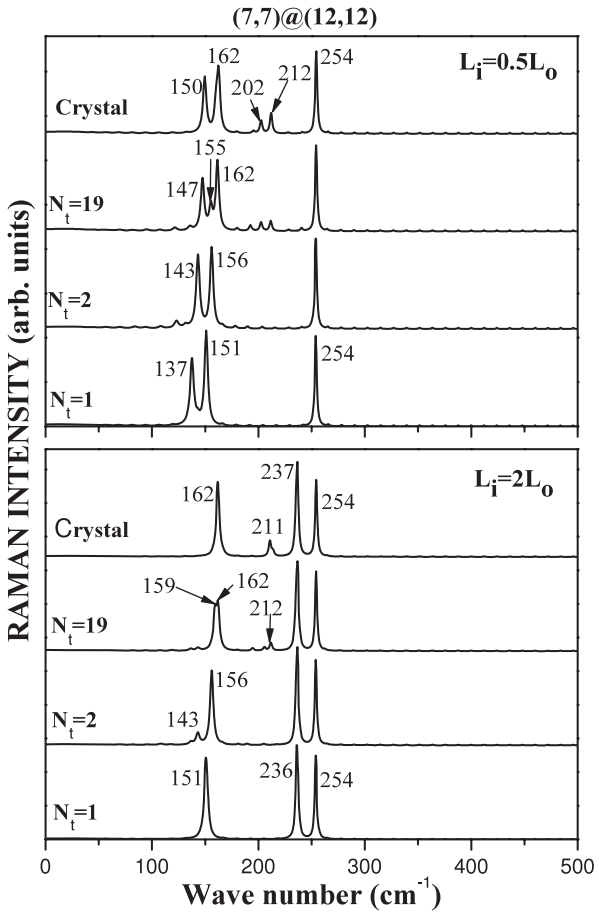

Figure 5. Dependence of the BLM range of (7, 7)@(12, 12) DWCNTs in terms of the number of tubes in the bundle for $L_i = 0.5L_o$ (top) and $L_i = 2L_o$ (bottom). The number of tubes is 1, 2, 19 and infinity.

123 and 191 cm^{-1} are in-phase and out-of-phase collective motions of both layers, respectively. In comparison with the Raman spectrum of the related SWNCTs, it can be pointed out that the BLMs of DWCNTs are characterized by an upshift of the modes. For $L_i = 0.5L_o$, the lowest frequency RBLM is upshifted, independently of the diameter of the tube: $\Delta\omega_{LF} \approx 13$ cm^{-1} with respect to the frequency of the RBM of the related SWCNTs. By contrast, for $L_i = 2L_o$, the upshift of the highest frequency RBLM increases with increasing tube diameter: $\Delta\omega_{HF} = 13$ cm^{-1} for (5, 5)@(10, 10), $\Delta\omega_{HF} = 18$ cm^{-1} for (7, 7)@(12, 12) and $\Delta\omega_{HF} = 26$ cm^{-1} for (10, 10)@(15, 15).

3.2. DWCNT bundles

The dependence as a function of the L_i/L_o ratio of the polarized ZZ Raman spectrum of the (7, 7)@(12, 12) infinite bundle (called crystal in the following) is shown in figure 3. In the TLM region, no significant difference between the Raman spectra of individual DWCNTs (figure 1, bottom) and DWCNT bundles (figure 3, bottom) is found. By contrast, in the BLM range, significant changes are observed (figure 3, top). With respect to individual (7, 7)@(12, 12) tubes, the low-frequency RBLMs located at 137 and 151 cm^{-1} are upshifted to 150 and 162 cm^{-1}, respectively. In contrast, the high-frequency RBLMs are located at the same position (254 cm^{-1}) in isolated DWCNT and DWCNT crystal. In (7, 7)@(12, 12) crystal, new modes, labeled BBLM (for bundle breathing-like mode), appear in the 200–210 cm^{-1} range. For $L_i < L_o$, these additional modes are observed at 202 and 212 cm^{-1}. For $L_i > L_o$, the BBLM frequencies are at 211 and 214 cm^{-1} (unresolved band), respectively.

The calculated Raman spectra for the (5, 5)@(10, 10), (7, 7)@(12, 12) and (10, 10)@(15, 15) DWCNT crystals are shown in the BLM region for $L_i = 0.5L_o$ (figure 4, top) and $L_i = 2L_o$ (figure 4, bottom), respectively. These spectra can be compared with those of individual DWCNTs (figure 2). For both the L_i/L_o ratios, the relative intensity of the BBLMs increases with the diameter of the nanotube. For all the tubes investigated, the lowest-frequency radial breathing modes are upshifted with respect to their positions in the related individual DWCNT. In contrast, the highest-frequency modes are at the same positions as in individual and DWCNT bundles. This result underlines the weak effect of DWCNT–DWCNT interaction for the modes associated with the inner tubes.

Finally, we were interested with the dependence on the Raman spectrum of the number of tubes in a bundle for different L_i/L_o ratio. In order to illustrate this dependence we discuss the Raman spectra of the (7, 7)@(12, 12) DWCNT for

$L_i = 0.5L_o$ (figure 5, top) and $L_i = 2L_o$ (figure 5, bottom). These results can be compared with those in figure 6 of [18] obtained for $L_i = L_o$. For $L_i > L_o$ (figure 5, bottom), the same behavior as that for $L_i = L_o$ is found for all the RBLMs [18]. An additional peak at 237 cm^{-1}, assigned to the radial breathing mode of the part of the inner tube which does not interact with the outer tube, is found in the spectra. Its position is independent of the size of the bundle. For $L_i < L_o$ (figure 5, top), as well the mode assigned to the radial breathing mode of the part of the outer tube which does not interact with the inner tube (150 cm^{-1} for individual tube) the lowest frequency RBLM significantly upshifts with the number of tubes in the bundle. Concerning the additional modes in the 200–214 cm^{-1} range, their intensity increases with the size of the bundle as expected.

4. Conclusion

In conclusion, we have performed a detailed numerical study of the Raman spectra of individual DWCNTs and DWCNT bundles as a function of the relative lengths of the inner (L_i) and outer (L_o) tubes. Thanks to the spectral moments method, we have investigated DWCNTs with length greater than 250 nm and bundles consisting of more than 100 DWCNTs. Important finite-size effects (length and number of nanotubes) are observed essentially in the BLM region with additional modes predicted. These modes must be considered in the analysis of experimental data.

Acknowledgments

The computations were performed at CINES (Montpellier, France). The work was supported by a CNRS-France/CNRST-Morocco agreement.

References

[1] Iijima S 1991 *Nature* **354** 56
[2] Dresselhaus M S and Eklund P C 2000 *Adv. Phys.* **49** 705
[3] Rao A M, Richter E, Bandow S, Chase B, Eklund P C, Williams K A, Fang S, Subbaswamy K R, Menon M, Thess A, Smalley R E, Dresselhaus G and Dresselhaus M S 1997 *Science* **275** 187
[4] Kürti J, Kresse G and Kuzmany H 1998 *Phys. Rev.* B **58** R8869
[5] Sánchez-Portal D, Artacho E, Soler J M, Rubio A and Ordejón P 1999 *Phys. Rev.* B **59** 12678
[6] Benoit C, Royer E and Poussigue G 1992 *J. Phys.: Condens. Matter* **4** 3125
[7] Rahmani A, Benoit C and Poussigue G 1994 *J. Phys.: Condens. Matter* **6** 1483
[8] Rahmani A, Sauvajol J L, Rols S and Benoit C 2002 *Phys. Rev.* B **66** 125404
[9] Sugai T, Omote H, Bandow S, Tanaka N and Shinohara H 2000 *J. Chem. Phys.* **112** 6000
[10] Flahaut E, Peigney A, Laurent Ch and Rousset A 2000 *J. Mater. Chem.* **10** 249–52
[11] Zhu H, Xu C, Wei B and Wu D 2002 *Carbon* **40** 2021–41
[12] Bandow S, Chen G, Sumanasekera G U, Gupta R, Yudasaka M, Iijima S and Eklund P C 2001 *Chem. Phys. Lett.* **337** 48
[13] Bacsa R, Peigney A, Laurent C, Puech P and BacsaW S 2002 *Phys. Rev.* B **65** 161404(R)
[14] Bandow S, Takizawa M, Hirahara H, Yudasaka M and Iijima S 2002 *Phys. Rev.* B **66** 075416
[15] Ci L, Zhou Z, Yan X, Liu D, Yuan H, Song L, Wang J, Gao Y, Zhou J, Zhou W, Wang W and Xie S 2003 *J. Phys. Chem.* B **107** 8760
[16] Cambedouzou J, Sauvajol J L, Rahmani A, Flahaut E, Peigney A and Laurent C 2004 *Phys. Rev.* B **69** 235422
[17] Pfeiffer R, Kuzmany H, Kramberger Ch, Schaman Ch, Pichler T, Kataura H, Achiba Y, Kürti J and Zólyomi V 2003 *Phys. Rev. Lett* **90** 225501
[18] Rahmani A, Sauvajol J L, Cambedouzou J and Benoit C 2005 *Phys. Rev.* B **71** 125402
[19] Dobardžić E, Maultzsch J, Milošević I, Thomsen C and Damnjanović M 2003 *Phys. Status Solidi* b **237** R7
[20] Popov V N and Henrard L 2001 *Phys. Rev.* B **63** 233407
[21] Popov V N and Henrard L 2002 *Phys. Rev.* B **65** 235415
[22] Rahmani A, Benoit C, Jullien R, Poussigue G and Sakout A 1996 *J. Phys.: Condens. Matter* **8** 5555
[23] Rahmani A, Benoit C, Jullien R, Poussigue G and Sakout A 1997 *J. Phys.: Condens. Matter* **9** 2149
[24] Rahmani A, Jund P, Benoit C and Jullien R 2001 *J. Phys.: Condens. Matter* **13** 5413
[25] Henrard L, Hernández E, Bernier P and Rubio A 1999 *Phys. Rev.* B **60** R8521